Early Cretaceous magnetic stratigraphy in the APTICORE drill core and adjacent outcrop at Cismon (Southern Alps, Italy), and correlation to the proposed Barremian-Aptian boundary stratotype

J.E.T. Channell*
Department of Geological Sciences, University of Florida, P.O. Box 112120, Gainesville, Florida 32611, USA

E. Erba
Dipartimento di Scienze della Terra, Università di Milano, 20133 Milano, Italy

G. Muttoni
Institut für Geophysik, ETH Hönggerberg, 8093 Zürich, Switzerland

F. Tremolada
Dipartimento di Scienze della Terra, Università di Milano, 20133 Milano, Italy

ABSTRACT

Lower Cretaceous mainly white and/or gray pelagic cherty limestones have been sampled in the APTICORE drill core and in the adjacent outcrop at Cismon, Southern Alps, Italy. Magnetic polarity stratigraphy of the drill core indicates that the top of the section is in the Cretaceous long normal polarity interval, 26 m above the reverse polarity zone correlative to polarity chron CM0. The base of the drilled section, at a stratigraphic depth of 116.71 m, is in a reverse polarity zone correlative to CM9. The coeval stratigraphic interval has been sampled in the adjacent outcrop in order to tie the drill core record to the outcrop. The correlation of polarity zones to polarity chrons is aided by the known correlation of nannofossil events to polarity chrons in other Italian land sections. New magnetostratigraphic sampling of the proposed Barremian-Aptian boundary stratotype section at Gorgo a Cerbara (Umbria, Italy) improves the definition of CM0 in this section and facilitates correlation to Cismon. Revised nannofossil biostratigraphy based on quantitative analyses greatly increases the stratigraphic resolution of the Barremian-Aptian boundary interval both at the proposed boundary stratotype (Gorgo a Cerbara) and at Cismon.

*E-mail: jetc@nersp.nerdc.ufl.edu.

Keywords: Cretaceous, Italy, nannofossils, paleomagnetism, stratigraphy.

INTRODUCTION

The magnetic and biostratigraphy of the ~400 m Hauterivian to Campanian section located on the west bank of the Cismon River at lat 46.04°N, long 11.76°E (Fig. 1), was originally documented by Channell et al. (1979). At the time, the M-sequence (Early Cretaceous) magnetic stratigraphy in the predominantly gray thin-bedded pelagic limestone section was not interpretable prior to polarity chron CM3 (earliest Barremian) due to the poor pattern fit of polarity zones to the oceanic magnetic anomaly record of Larson and Hilde (1975). The interpretation of pre-CM3 polarity chrons was facilitated by subsequent nannofossil biostratigraphy (Bralower, 1987) at Cismon, and in Umbrian (North Apennine) sections where magnetic stratigraphies were established by Lowrie and Alvarez (1984). On the basis of these studies, Bralower (1987) suggested that the magnetic stratigraphy in the Cismon outcrop extended back to CM10N (early Hauterivian). Following Helsley and Steiner (1969), who first postulated the existence of the Cretaceous long normal polarity interval, the Cismon section provided its first documentation in a single stratigraphic section (Channell et al., 1979). The overlying Campanian to Paleocene magnetic stratigraphy and biostratigraphy at Cismon were documented by Channell and Medizza (1981). Recent magnetostratigraphic sampling of the CM8–CM10N (Hauterivian) interval of the Cismon section (Mayer, 1997) has not amended earlier studies.

The Cismon section was selected as the best possible reference section for the APTICORE Program, the mission of which is to document the record of mid-Cretaceous greenhouse climatic warming (Erba and Larson, 1998). The need for a continuous, uninterrupted section for biostratigraphy, cyclostratigraphy, and geochemical studies led to the drilling of a single 131.8-m-long bore hole through the middle Aptian to lower Hauterivian section (Erba and Larson, 1998; Erba et al., 1999). Drilling was carried out in December 1995 and January 1996. The core recovery was essentially 100% with a core diameter of 11 cm. The hole was then reamed to 20 cm diameter for geophysical logging.

The preliminary lithologic description of cores was carried out at the drill site (see Erba and Larson, 1998; Erba et al., 1999). Cores were sectioned in 1 m lengths, packed in wooden crates, and transported to Milan for additional lithologic description, whole-core magnetic susceptibility measurements, core splitting, and subsampling. Prior to splitting, susceptibility measurements at 5 cm intervals downcore were carried out with a Bartington MS2 susceptibility bridge and a 15-cm-diameter sensing loop. The cores were not azimuthally oriented in situ at the drill site; however, dip of the bedding, which varies from 17° to 55° downdip to the south (Table 1),

GSA Bulletin; September 2000; v. 112; no. 9; p. 1430–1443; 13 figures; 4 tables.

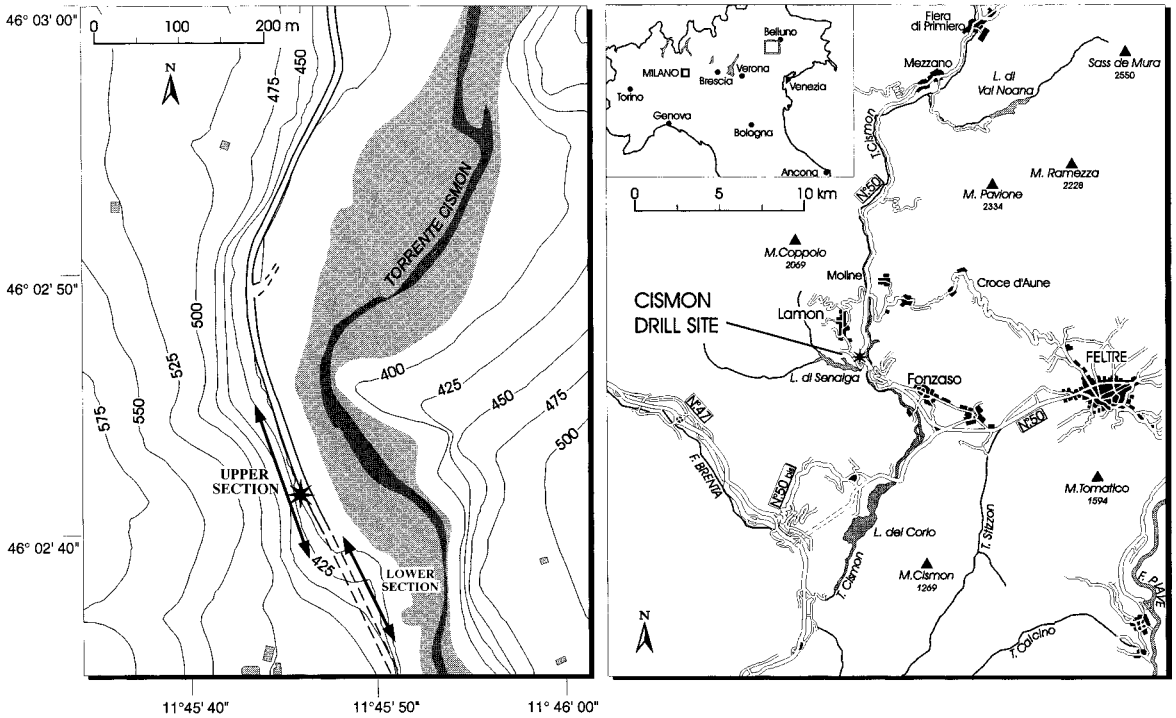

Figure 1. Location map for the Cismon drill site (asterisk) and the upper and lower outcrop sections. The road is marked as a double solid line; the road tunnel is marked as a dashed line. The upper section is on the west side of the road and the lower section is on the east side of the road tunnel. The flood plain of the Cismon River (Torrente Cismon) is shaded (map after Erba and Larson, 1998).

TABLE 1. APTICORE DRILL CORE

Interval		Bedding dip
mbwh*	Stratigraphic depth	
00.00–64.62	00.00–61.13	19°
64.62–66.15	61.13–62.21	45°
66.15–72.15	62.21–67.13	35°
72.15–74.82	67.13–68.84	50°
74.82–82.54	68.84–75.53	30°
82.54–86.93	75.53–78.05	55°
86.93–101.72	78.05–89.38	40°
101.72–113.78	89.38–100.30	25°
113.78–126.40	100.30–111.55	27°
126.40–131.80	111.55–116.71	17°

*Meters below well head.

allowed the cores to be oriented in azimuth after recovery. The cores were split along the dip line, and 2.5-cm-diameter cylinders were drilled perpendicular to the split surface of the eastern (working) half of the core at 20–30 cm intervals. All cylindrical samples were therefore assigned an azimuth of 90°E and a dip of zero. Downhole logs indicated that the borehole did not deviate by more than 2° from the vertical. Bedding tilt correction to the magnetic remanence directions was performed by utilizing dip measurements determined from the recovered drill core and bedding strikes measured in the coeval outcrop. The 2.5-cm-diameter cylinders were trimmed to lengths of 2.3 cm and the end pieces were labeled and sent to colleagues for biostratigraphic and stable isotope analyses, ensuring unambiguous correlation of the resulting data with the magnetic stratigraphy.

MAGNETIC POLARITY STRATIGRAPHY

Cylindrical samples were selected at 30–40 cm intervals downcore for determination of the magnetic polarity stratigraphy. After measurement of the natural remanent magnetization (NRM), which had values in the 0.1–1 mA/m range, stepwise thermal demagnetization was carried out from 100 to 500 °C in 25 °C steps and from 500 to 560 °C in 15 °C steps. After demagnetization at ~200 °C, a characteristic magnetization component is isolated as indicated by a linear trend to the origin of the orthogonal projections (Fig. 2). Component directions were determined by visual selection of the linear portion of each orthogonal projection defining the characteristic high blocking temperature component, and using the standard least-squares method (Fig. 3A; Kirschvink, 1980). In Figure 4, the component declination and inclination are plotted against stratigraphic depth. The maximum angular deviation (MAD) values $<10°$ indicate that the components are generally well defined. Stratigraphic depths were computed from the distance below well head (mbwh) and bedding dip estimates were determined from the recovered core (Table 1).

In the more than 20 years since the original magnetostratigraphic sampling of the outcrop at Cismon (Channell et al., 1979), the outcrop markings have disappeared. For this reason, we resampled the outcrop coeval with the section recovered in the drill core in order to provide a means of correlation from the drill core to the outcrop. The coeval outcrop at Cismon is divided into a stratigraphically upper and lower section separated by the road tunnel entrance (Fig. 1). The upper section lies in the road cut on the western side of the road, and the lower section lies along an unpaved track to the east of the road tunnel along the bank of the Torrente (river) Cismon (Fig. 1). The top of the lower section is approximately at the same stratigraphic level as the base of the upper section. The join between the two sections is in the upper Barremian (polarity chron CM1n).

Samples were collected in the outcrop with a hand-held gasoline-powered drill. The stratigraphic distance between samples was dictated by the quality of the outcrop and the degree of exposure. Samples were generally

collected each 20–30 cm stratigraphically along the section; however, this interval was not achieved everywhere, particularly in the upper section where exposure is discontinuous. An arbitrary zero level was placed on the outcrop at a level estimated to be close to the base of the drill-core section. Each meter is indicated in blue paint on the outcrop so that these levels can be identified for future studies that may require magnetostratigraphic age control.

For the upper section, 24 of the 74 samples were stepwise demagnetized using alternating fields in the 5–100 mT peak field range. The remaining samples from the upper section and all samples from the lower section were thermally demagnetized. After measurement of the natural remanent magnetization (NRM), stepwise thermal demagnetization was carried out in 50 °C steps from 100 to 300 °C and in 25 °C steps from 300 to 575 °C. Orthogonal projections of thermal demagnetization data (Fig. 5) indicate that the characteristic component is defined after demagnetization at ~200 °C. The maximum unblocking temperature of ~575 °C indicates that magnetite is carrier of the NRM. Alternating field demagnetization of samples from the upper section (Fig. 5) indicates that the characteristic magnetization component can be demagnetized in peak fields greater than ~50 mT, again indicative of a low coercivity (magnetite) remanence carrier (see review of magnetic properties of Italian Cretaceous pelagic limestones by Channell and McCabe, 1994). Component directions were determined by visual selection of linear portions of each orthogonal projection, and then using the standard least-squares method (Kirschvink, 1980) to compute the component direction (Fig. 3, B and C). In Figure 6, the component declination and inclination are plotted against stratigraphic depth for the lower and upper sections. The maximum angular deviation (MAD) values of $<10°$ indicate that the components are generally well defined. Virtual geomagnetic pole (VGP) latitudes for the drill core and the outcrop (Fig. 7) provide correlation among the three sections.

The data for the drill core and the lower outcrop pass the reversal test at the 95% confidence level, with a classification at the boundary between A and B (see McFadden and McElhinny, 1990). The test is indeterminate for the upper section due to insufficient (reverse polarity) data. The drill-core characteristic magnetization components are more scattered than those from the lower and upper outcrop sections (Fig. 3; Table 2). The scatter of component directions in the drill core is largely in declination (Fig. 3A) and is therefore attributable to errors in azimuthal orientation of the drill core. Azimuthal orientation of the drill core was determined by observation of the bedding dip direction in the recovered core. The bedding dip varies from 17° to 55° (Table 1) and the azimuthal uncertainty in core orientation increases as bedding dip decreases.

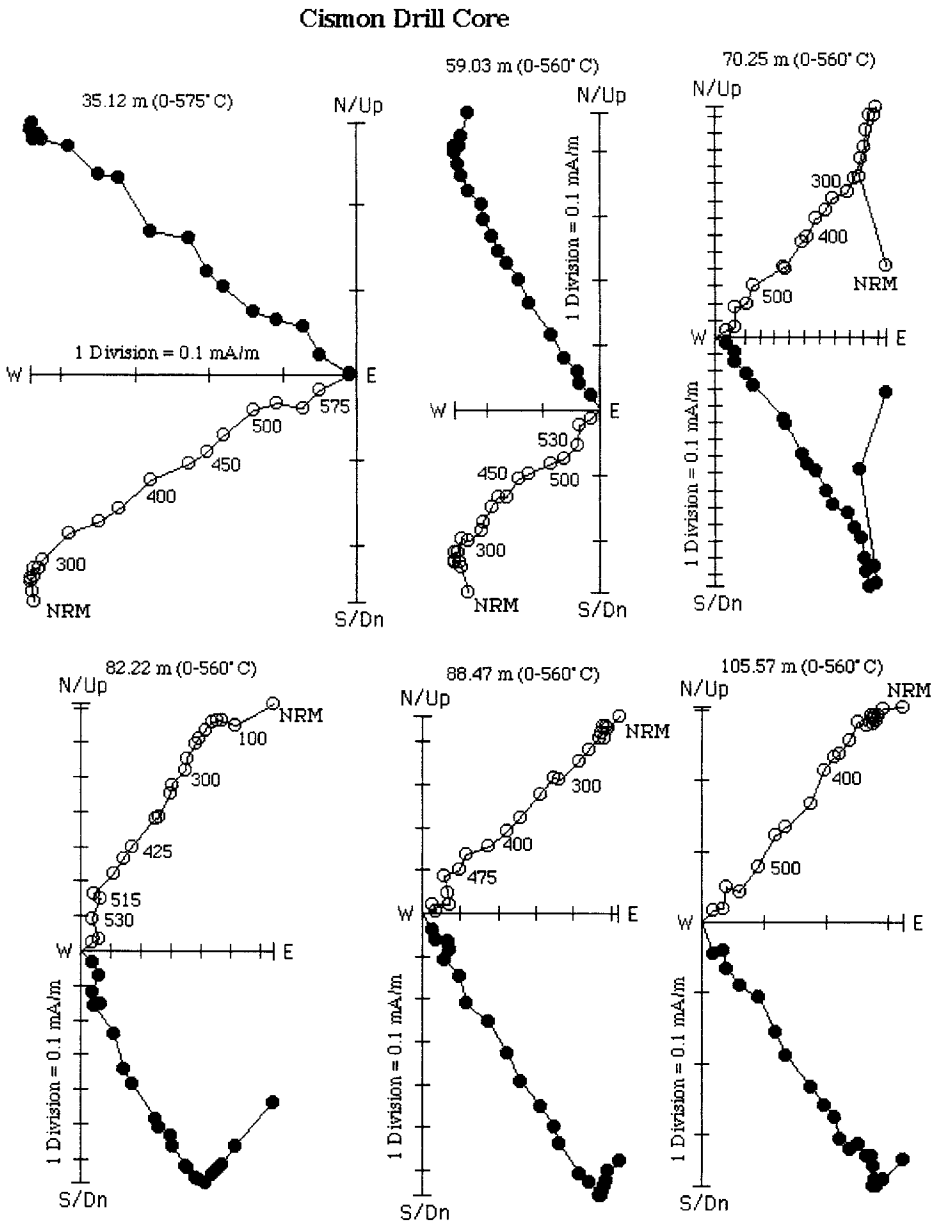

Figure 2. Orthogonal projection of thermal demagnetization data from the Cismon drill core. Directions corrected for bedding tilt. Open and closed symbols represent projection of the vector end point on the vertical and horizontal planes, respectively. The stratigraphic depth in the drill core and the demagnetization range is indicated for each sample. The temperature in degrees Celsius is indicated for some steps.

CORRELATION OF POLARITY ZONES TO BIOSTRATIGRAPHIC EVENTS

The correlation of nannofossil events to polarity chrons for the Hauterivian to Aptian has been established from numerous Italian pelagic limestone sections in the Southern Alps and Umbria (e.g., Channell et al., 1979, 1987, 1995b; Bralower, 1987; Channell and Erba,

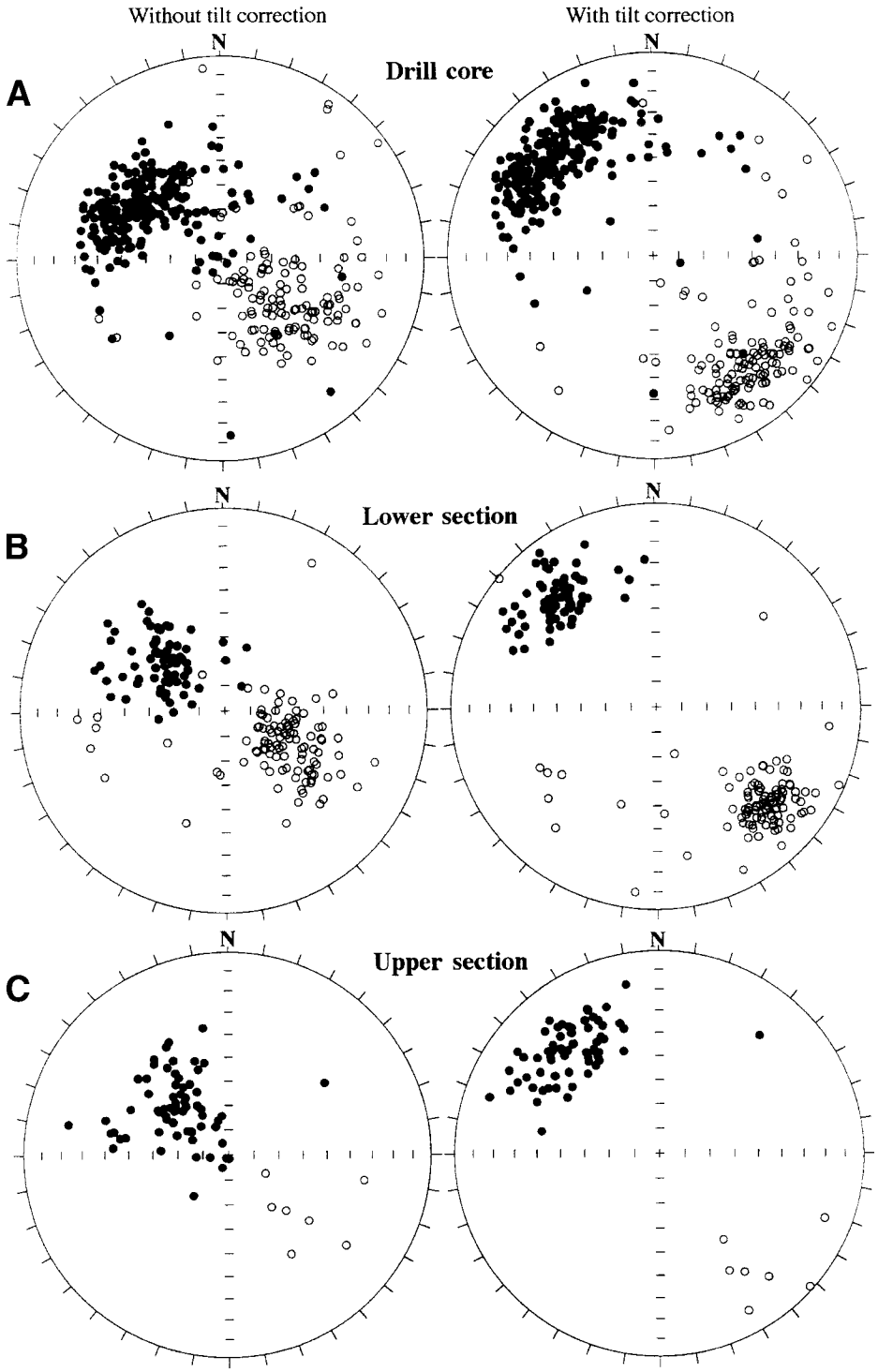

Figure 3. Equal-area projection of the characteristic magnetization components at Cismon with (right) and without (left) bedding tilt correction for (A) the drill core, (B) the lower outcrop section, and (C) the upper outcrop section. The increased azimuthal scatter of the component for the drill core can be attributed to poorly constrained azimuthal orientation of the drill core.

1992). In sections characterized by fairly constant sedimentation rates, the pattern of polarity zones can be matched to the geomagnetic polarity time scale (GPTS) to identify polarity chrons. The process is aided by the presence of biostratigraphic events with known correlation to polarity chrons. The continuous record of the Cismon core for the upper Hauterivian to lower upper Aptian allowed recognition of several biostratigraphic events based on calcareous nannofossils, planktonic foraminifers, radiolarians, and dinoflagellates (see Erba et al., 1999). All the standard nannofossil events previously calibrated to polarity chrons in low-latitude sections were identified. Additional events based on quantitative analyses of nannofloras greatly improved the stratigraphic resolution.

The nannoconid crisis has been dated in various land sections and deep-sea cores as younger than CM0 and slightly older than the oceanic anoxic subevent 1a (Erba, 1994). In the Cismon drill core, the nannoconid crisis occurs below the base of the Selli (black shale) Level and above the polarity zone correlative to CM0 (Fig. 8). The same stratigraphic position for this event has been observed in other Italian sections (Fig. 9) as well as in Deep Sea Drilling Project and Ocean Drilling program cores from the Pacific and Atlantic Oceans (Erba, 1994; Bralower et al., 1994).

In the Cismon drill core the first occurrence (FO) of *Rucinolithus irregularis* is just prior to polarity chron CM0 (Fig. 8), consistent with its position in other Italian sections (Fig. 9). The FO of *Nannoconus truittii* in the Cismon drill core also is just prior to CM0 (Fig. 8) and was reported at similar or slightly younger levels (within CM0) in other Italian sections (Fig. 9). We attribute the significantly older first occurrence in the Capriolo and Cismon outcrops (Bralower, 1987) as due to contamination or taxonomic discrepancy. The FO of *N. truittii* has not previously been utilized in magnetobiostratigraphic correlations; however, it is potentially very useful due to its common occurrence in marginal to oceanic settings at low and high latitudes.

In the Cismon drill core, changes in nannoconid abundance and characteristics are recognized in the vicinity of CM0 (Fig. 8), providing additional means of correlation to other sections. In particular, a marked decrease in abundance of narrow-canal nannoconids (named nannoconid decline) precedes CM0 and is correlatable with the FO of *R. irregularis.* This nannoconid decline has been observed in other Italian sections (Fig. 9) and oceanic sites (Erba, 1994). In the Cismon drill

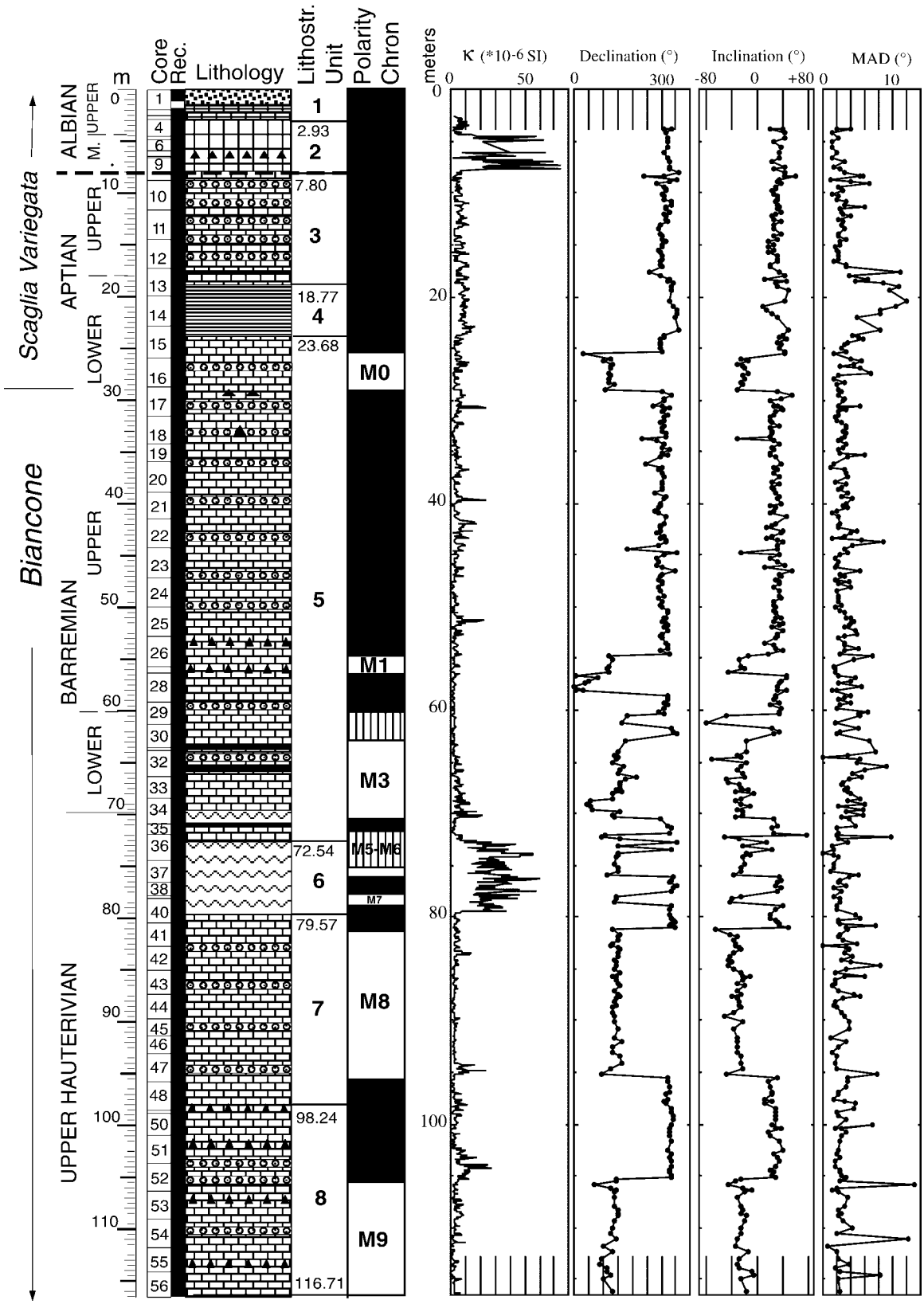

Figure 4. Cismon drill core: volume susceptibility (κ), component declination, inclination, and maximum angular deviation (MAD) values are plotted against stratigraphic depth with identification of polarity chrons. MAD values of zero indicate that the component magnetization direction was based on a stable end point, rather than the least-squares fit of a linear trend on the orthogonal projection. Lithostratigraphic units: 1—gray limestone and black shale; 2—red limestone, marlstone, and red chert; 3—gray limestone and

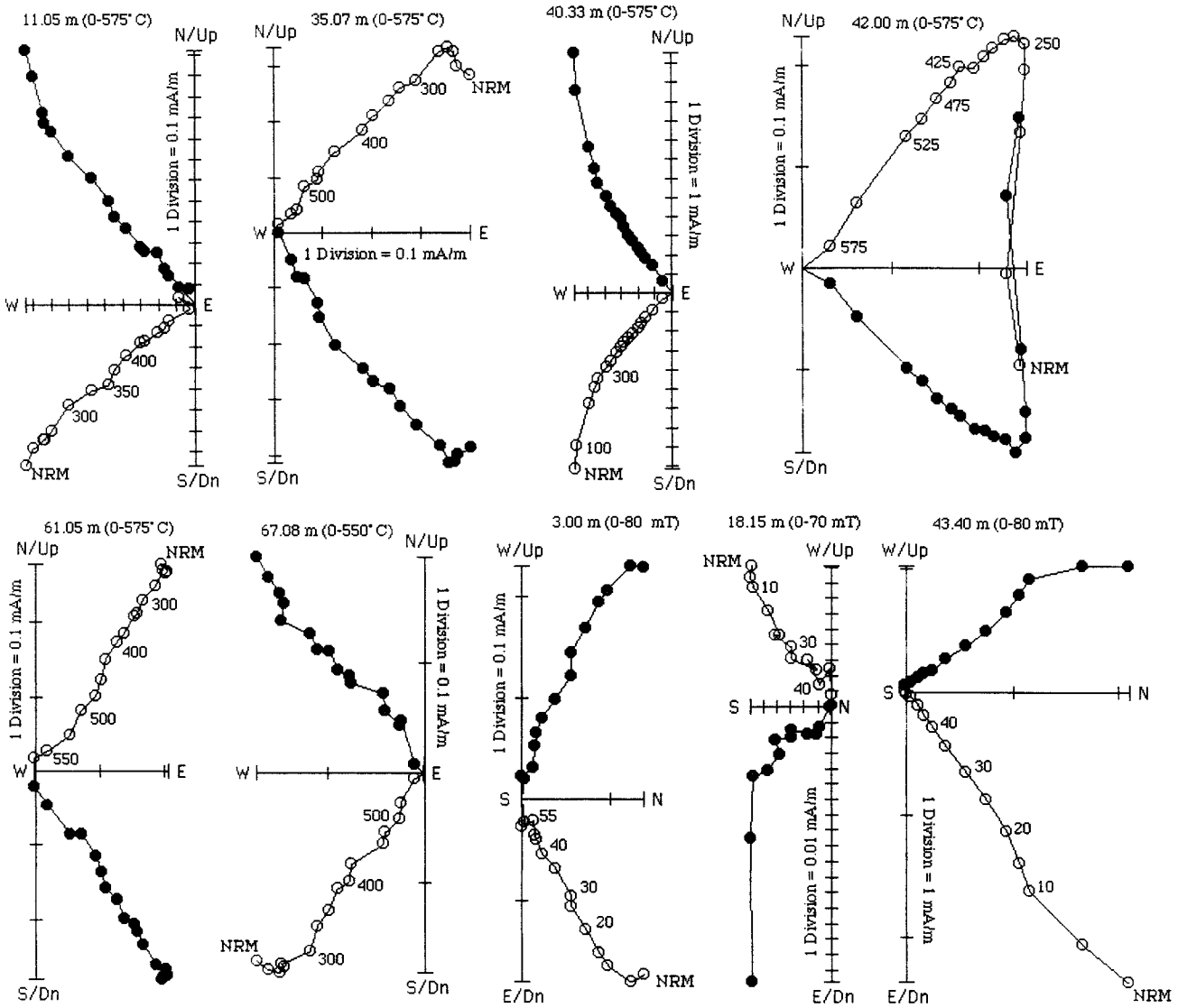

Figure 5. Cismon outcrop: orthogonal projection of thermal demagnetization data for the lower section, and alternating field (AF) demagnetization data for the upper section. Directions corrected for bedding tilt. Open and closed symbols represent projection of the vector end point on the vertical and horizontal planes, respectively. The stratigraphic position and the demagnetization range are indicated for each sample. The temperature in degrees Celsius and peak AF in mT are indicated for some steps.

core, the nannoconid abundance decreases within CM0 to a level where, for the first time, the wide-canal nannoconids become more abundant than the narrow-canal nannoconids (Fig. 8). Quantitative analyses of nannofloras have revealed the same change within CM0 in other Italian sections (Fig. 9) and deep-sea cores (Erba, 1994).

The identification of CM3 in the Cismon drill core is supported by the position of two nannofossil events, namely the last occurrences (LOs) of *Calcicalathina oblongata* and *Lithraphidites bollii.* These two nannofossil events have consistent occurrence relative to polarity chrons in numerous Italian sections (Fig. 9). Similarly, the FO of *Rucinolithus terebrodentarius* and the LO of *Cruciellipsis cuvillieri* generally occur in the CM7–CM8 interval and CM8, respectively, permitting identification of these polarity chrons in the Cismon drill core.

Quantitative investigations of Hauterivian nannofloras at Cismon indicate that the acme of pentaliths (*Micrantholithus* and *Braarudosphaera*) is close to 76.0 m in the Cismon drill core. This peak has been identified close to the onset of CM5 in the Breggia wall section

radiolarian beds and nodules; 4—Selli level (mainly black shale); 5—light gray limestone with radiolarian beds and nodules and rare chert lenses; 6—red pseudonodular limestone; 7—light gray limestone with radiolarian beds and nodules and chert lenses; 8—light gray limestone with radiolarian beds, nodules and chert layers. Brick pattern—gray pelagic limestone; black triangles—chert; circles—radiolarian beds; thick black lines—black shale beds. The lithologic log is after Erba and Larson (1998) and Erba et al. (1999).

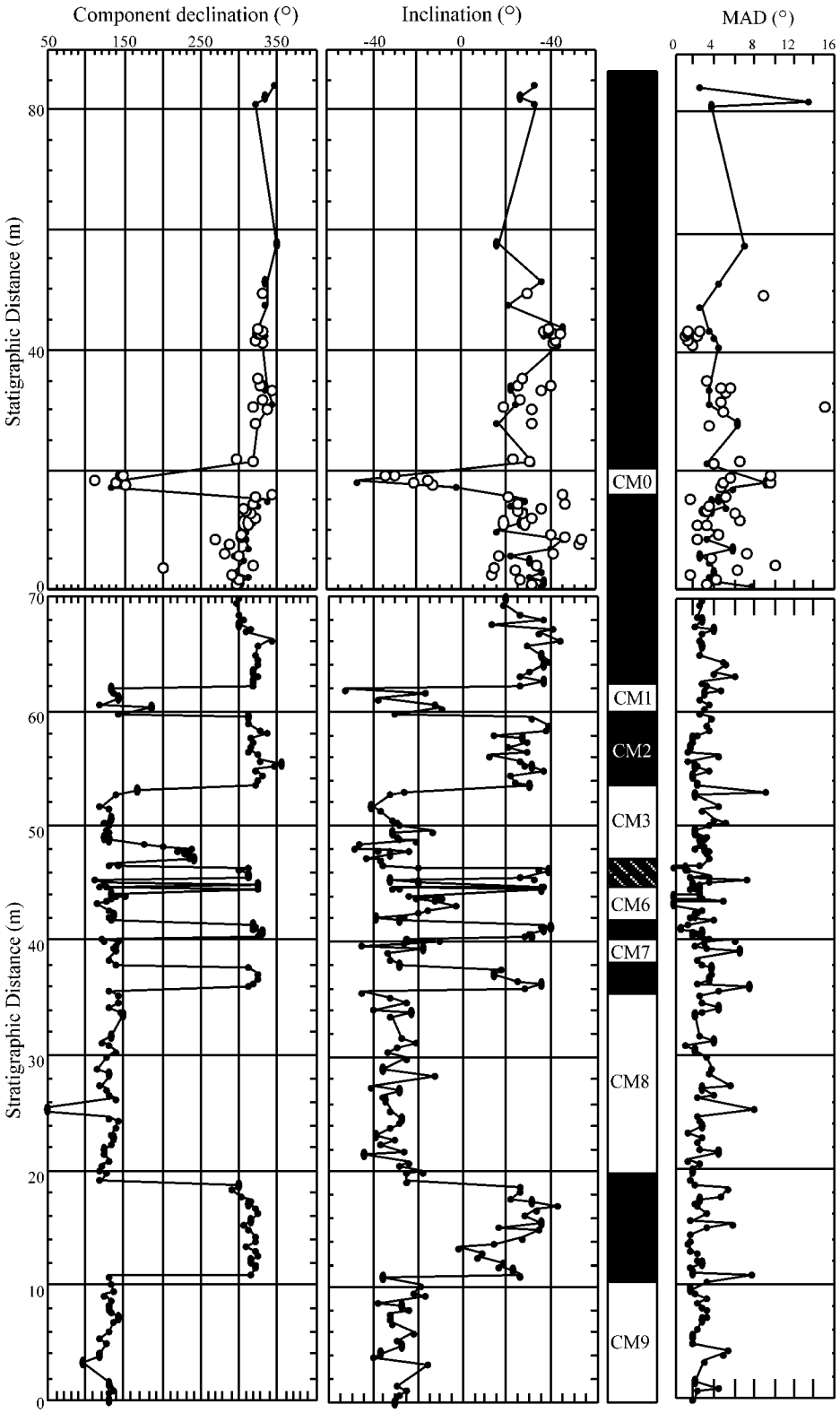

(Fig. 10; unpublished data augmenting original study of Breggia wall section by Channell et al., 1993). The end of the acme of pentaliths occurs in the 72–73 m interval in the Cismon drill core and in CM5 at the Breggia wall section (Fig. 10). The presence of *L. bollii* at the base of the Cismon drill core indicates that the reverse polarity zone at the base of the section correlates to CM9 rather than an older polarity chron (Fig. 9).

The meter levels of polarity zone boundaries in the drill core and in outcrop, and the correlation of polarity zones to polarity chrons, are given in Table 3.

PROPOSED BARREMIAN–APTIAN BOUNDARY STRATOTYPE AT GORGO A CERBARA

The Gorgo a Cerbara section (northern Umbrian Apennines) comprises the Aptian–Albian Scisti a Fucoidi Formation overlying Maiolica Limestones (see Coccioni et al., 1992). The magnetic stratigraphy of the Gorgo a Cerbara section was studied by Lowrie and Alvarez (1984), who identified a sequence of polarity chrons from CM0 to CM10N in 180 m of stratigraphic section. Subsequently, the nannofossil and foraminiferal biostratigraphy of the Barremian–Aptian part of the section was documented by Coccioni et al. (1992). The importance of this section to chronostratigraphy was accentuated by ammonite finds (Cecca et al., 1994) documenting the first biostratigraphically useful sequence of ammonites to be found in a Maiolica section, allowing the section to be directly tied to ammonite zones and hence to Hauterivian and Barremian stage boundaries. Since this important discovery, ammonite finds were correlated to polarity chrons in other Maiolica sections of Valanginian to Aptian age from Umbria and the Southern Alps (Channell et al., 1995b). This allowed geologic stage boundaries and nannofossil events in this interval to be directly correlated to polarity chrons (and hence to each other) for the first time. Previously, the correlation of nannofossil events to stage boundaries relied essentially on the correlations of Thierstein (1973, 1976) from southern France augmented by a few ammonite-dated sections from Spain and France.

Figure 6. Component declination, inclination, and maximum angular deviation (MAD) values plotted against stratigraphic depth, with identification of polarity chrons for the upper and lower outcrops. MAD values of zero indicate that the component magnetization direction was based on a stable end point, rather than the least-squares fit of a linear trend on the orthogonal projection. For the upper section (top), closed symbols joined by line are component directions derived from alternating field (AF) demagnetization, and open symbols are derived from thermal demagnetization. For the lower section, all components were derived from thermal demagnetization data.

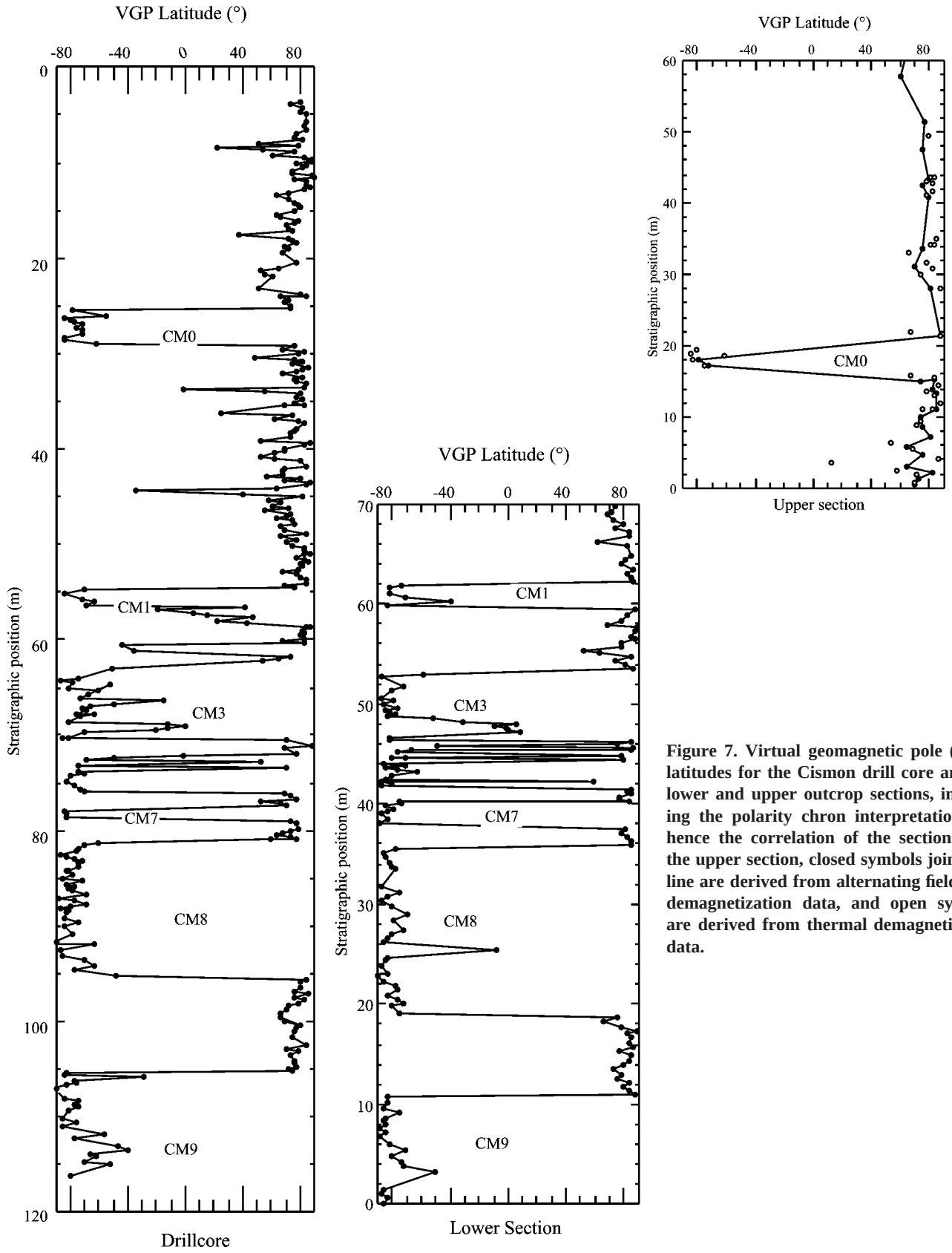

Figure 7. Virtual geomagnetic pole (VGP) latitudes for the Cismon drill core and the lower and upper outcrop sections, indicating the polarity chron interpretation and hence the correlation of the sections. For the upper section, closed symbols joined by line are derived from alternating field (AF) demagnetization data, and open symbols are derived from thermal demagnetization data.

Stratotype sections or stratotype boundary sections have rarely been redesignated in the history of the International Stratigraphic Commission. The only case of a stratotype boundary section that has been officially redesignated is the Miocene-Pliocene boundary stratotype at Capo Rossello (Sicily; Cita and Gartner, 1973).

A few years ago the Subcommission on Cretaceous Stratigraphy promoted the revision of all Cretaceous stages with the purpose of redefining the stage and substage boundaries and redesignating the boundary stratotypes. Within this framework, the Aptian working group selected the base of the polarity zone correlative to CM0 as the event defining the base of the Aptian stage and, therefore, the Barremian-Aptian boundary (Erba, 1996). As a consequence, the Gorgo a Cerbara section was proposed as a boundary stratotype for the base of the Aptian. Formal ratification of this proposal should take place in the near future. The decision placing the Barremian-Aptian boundary at the base of the polarity zone correlative to CM0 constitutes the first use of a magnetic polarity chron in the official definition of a geologic stage boundary. In view of the central role of geomagnetic polarity in the development of modern time scales (e.g., Cande and Kent, 1992; Channell et al., 1995a), it seems logical to continue this important initiative and revise the definition of other geologic stage boundaries to include their correlation to polarity chrons.

In order to improve the definition of CM0 at Gorgo a Cerbara, we resampled the interval originally sampled by Lowrie and Alvarez (1984), and correlated our samples to the original meter levels of Lowrie and Alvarez (1984; see Erba, 1996). Magnetization intensities are highly variable and close to magnetometer noise level. Component magnetizations, however, were resolved by thermal and alternating field demagnetization. The resulting directions were computed using the standard least squares method (Kirschvink, 1980). VGP latitudes were determined from the component directions (Fig. 11). We place the base of the polarity zone correlative to CM0 at 893.2 m, indistinguishable from the original designation by Lowrie and Alvarez (1984). The top of the polarity zone is at 895.2 m, about 70 cm higher in the section than the original designation. Intermediate component directions (VGPs) at the polarity chron boundaries probably indicate superimposed dual-polarity magnetization components where neither thermal nor AF demagnetization is successful in resolving individual magnetization components.

TABLE 2. MEAN MAGNETIZATION DIRECTIONS FOR THE DRILL CORE AND OUTCROP

	N	Dec (°)	Inc (°)	k	α_{95} (°)	Pole Lat (°N)	Pole Long (°E)	dp (°)	dm (°)
Core all*	343	304.3	54.9	10.6	2.5				
Core all†	343	317.0	31.6	11.8	2.3	44.2	257.3	1.6	2.9
Core normal polarity*	219	305.9	53.4	12.5	2.8				
Core normal polarity†	219	316.7	32.7	13.3	2.7				
Core reverse polarity*	124	121.1	–57.6	8.4	4.7				
Core reverse polarity†	124	137.6	–29.7	9.7	4.3				
Lower o/c all*	172	305.5	61.1	14.4	2.9				
Lower o/c all†	172	316.6	30.0	16.5	2.7	43.2	256.8	1.7	3.1
Lower o/c normal polarity*	70	309.1	58.0	27.6	3.3				
Lower o/c normal polarity†	70	318.9	28.5	34.9	2.9				
Lower o/c reverse polarity*	102	122.4	–63.2	11.1	4.4				
Lower o/c reverse polarity†	102	134.8	–31.0	12.2	4.2				
Upper o/c all*	74	312.7	61.1	13.1	4.7				
Upper o/c all†	74	319.6	32.0	16.4	4.2	46.0	254.8	3.1	5.5
Upper o/c normal polarity*	66	311.6	62.6	15.0	4.7				
Upper o/c normal polarity†	66	318.8	33.3	20.1	4.0				
Upper o/c reverse polarity*	8	139.1	–47.4	6.9	22.7				
Upper o/c reverse polarity†	8	145.7	–19.6	7.1	22.3				

Note: o/c—outcrop. Dec—declination. Inc—inclination.
*No tilt correction.
†With tilt correction.

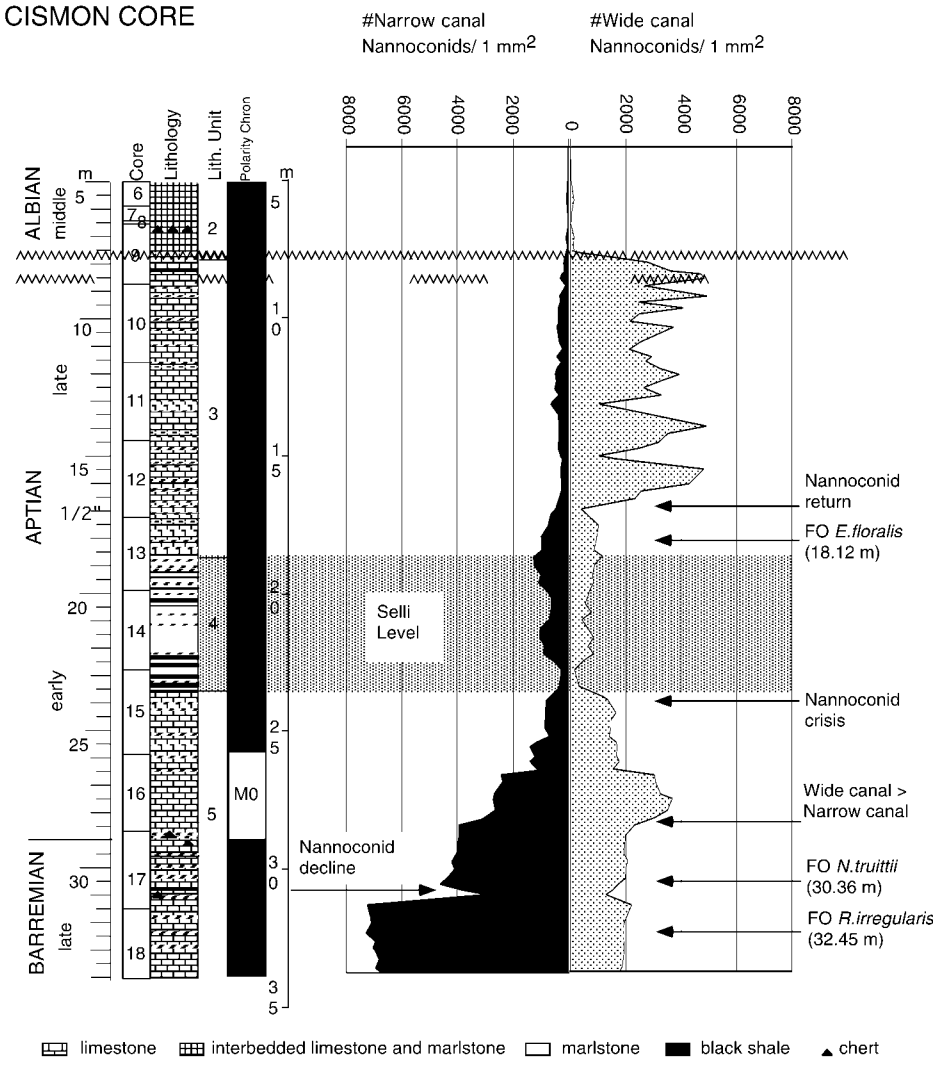

Figure 8. Absolute abundance (number of specimens per square millimeter of thin section) of narrow- and wide-canal nannoconids in the vicinity of CM0 in the Cismon drill core. Other first occurrence (FO) datums are indicated.

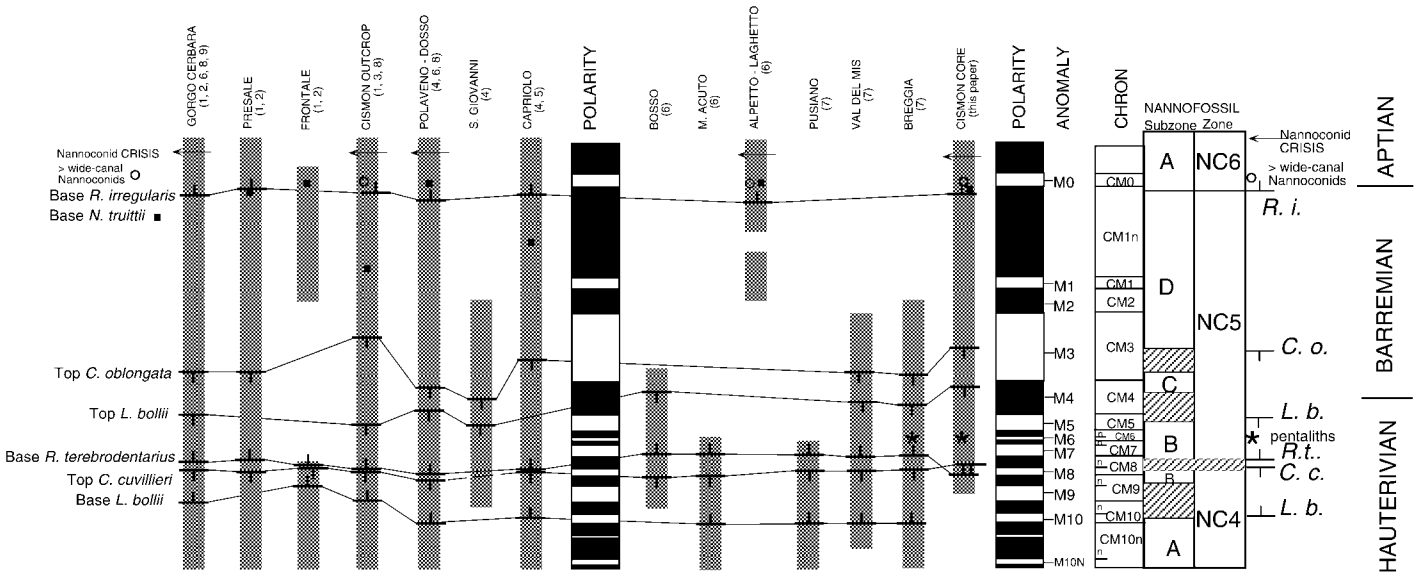

Figure 9. The correlation of nannofossil events to polarity chrons for Italian land sections from Umbria and the Southern Alps. The gray columns represent the analyzed interval for each individual section. The number in parentheses beneath the section name gives the reference: 1—Bralower (1987), 2—Lowrie and Alvarez (1984), 3—Channell et al. (1979), 4—Channell and Erba (1992), 5—Channell et al. (1987), 6—Channell et al. (1995b), 7—Channell et al. (1993), 8—Erba (1994), 9—Erba (1996).

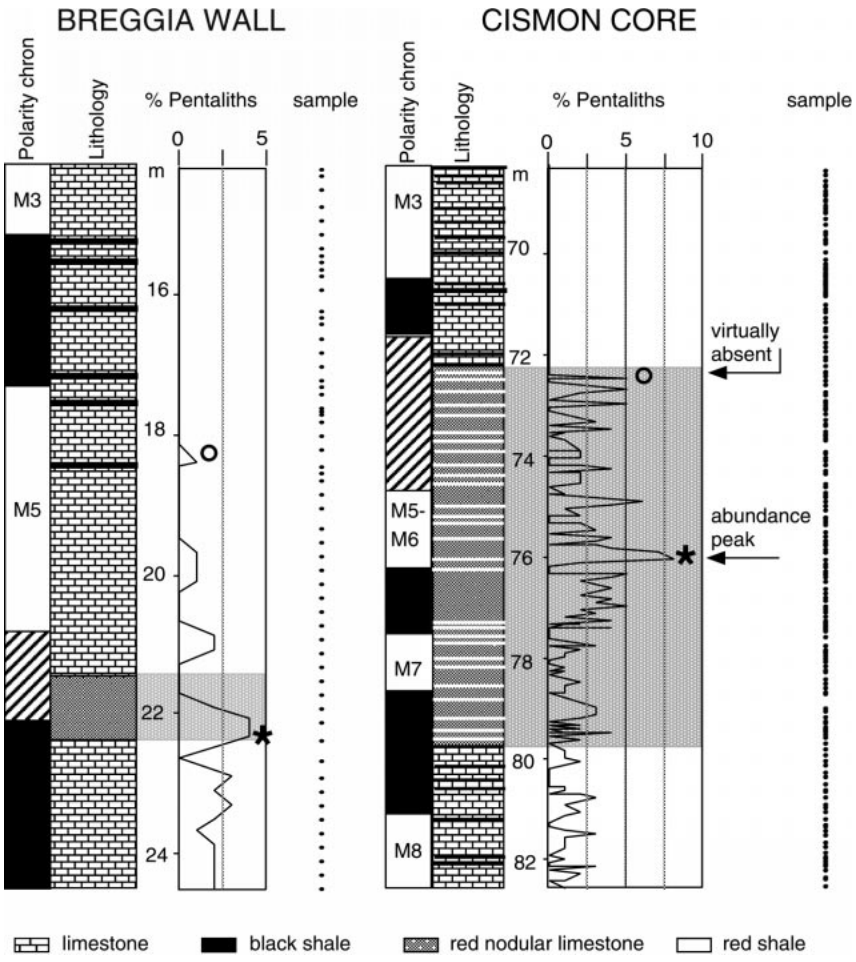

Figure 10. Percent pentaliths correlated to magnetic stratigraphy in the Cismon drill core and in the Breggia Wall section. The abundance peak of pentaliths (asterisk) correlates with red nodular limestones in both sections. Magnetic stratigraphy in the Breggia Wall section is from Channell et al. (1993).

TABLE 3. LOCATION OF POLARITY ZONE BOUNDARIES AND RESULTING SEDIMENTATION RATES WITHIN POLARITY CHRONS USING THE CENT94 TIME SCALE

Chron	Age (Ma)	Core (m)	Outcrop (m)	Core (m/Myr)	Outcrop (m/m.y.)
Top M0	120.60	25.75	90.00		
				8.6	10.0
Base M0	121.00	29.17	86.00		
				11.7	11.0
Top M1	123.19	54.68	62.04		
				5.2	6.8
Base M1	123.55	56.55	59.58		
				10.3	12.7
Top M3	124.05	61.7	53.22		
				5.4	5.0
Base M3	125.67	70.42	46.56		
				3.6	3.2
Base M6	127.23	76.1	41.61		
				6.1	5.2
Top M7	127.49	77.69	40.26		
				3.6	8.3
Base M7	127.79	78.76	37.77		
				8.5	7.2
Top M8	128.07	81.14	35.75		
				52.9	62.3
Base M8	128.34	95.42	18.92		
				35.2	28.6
Top M9	128.62	105.27	10.90		

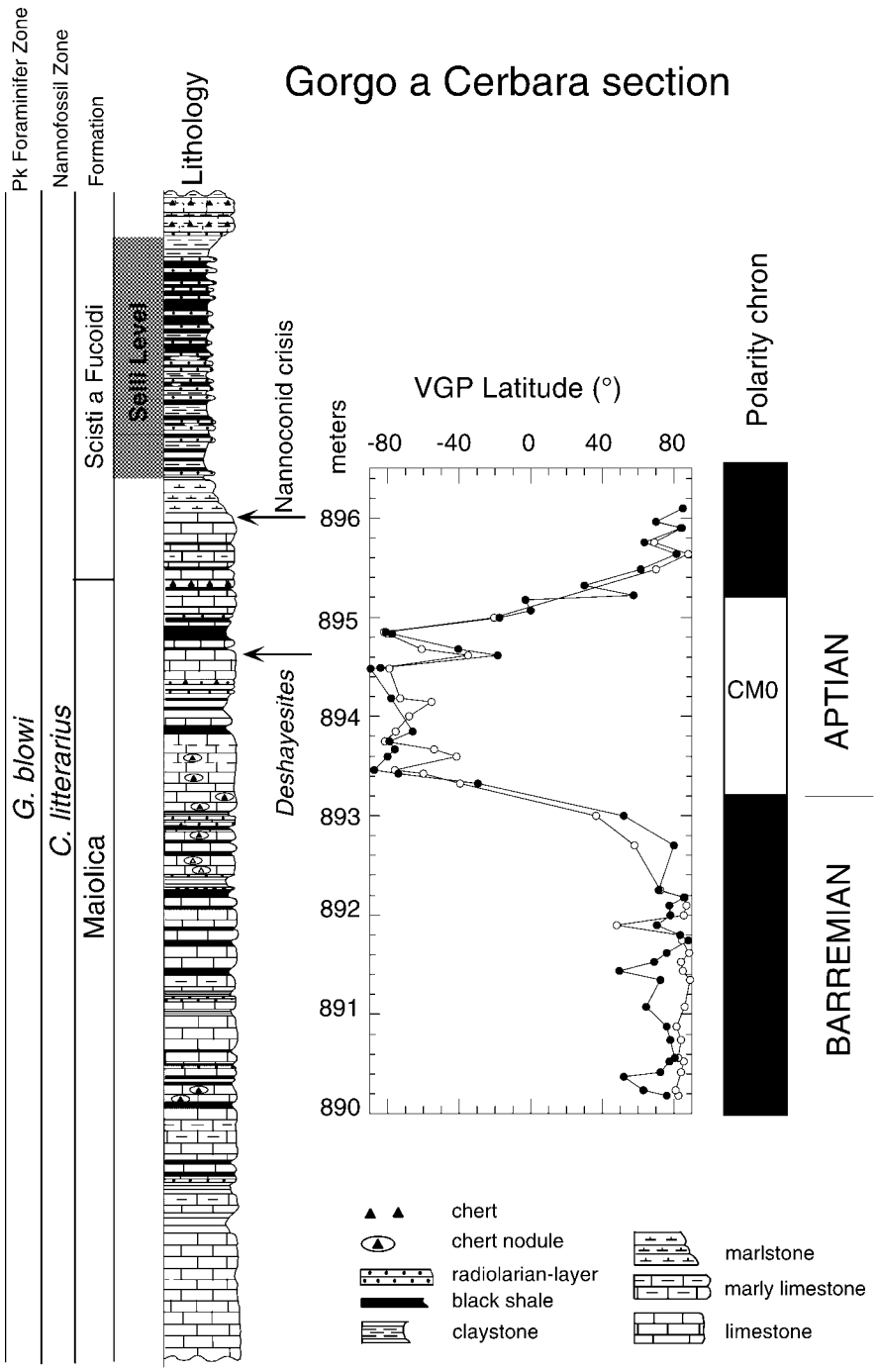

Figure 11. Virtual geomagnetic pole (VGP) latitudes at Gorgo a Cerbara, the proposed Barremian–Aptian boundary stratotype section. Open and closed symbols represent magnetization components defined by thermal and alternating field demagnetization, respectively. The Barremian-Aptian boundary has been designated to coincide with the base of polarity chron CM0 (at 893.2 m; see Erba, 1996). One ammonite specimen (*Deshayesites* sp.) was found within CM0 (Erba, 1996; Landra et al., 2000). The nannoconid crisis was identified at 895 m and the first occurrence (FO) of *R. irregularis* at 887 m. Meter levels follow those of Lowrie and Alvarez (1984), who originally documented the magnetic stratigraphy in this section.

Calcareous nannofossils have been quantitatively investigated in the upper Barremian–Aptian interval at Gorgo a Cerbara using the same methodology (see Erba, 1994) applied to the Cismon core. In the Gorgo a Cerbara section (Fig. 12), the nannoconid crisis is at the base of the lower critical interval (Coccioni et al., 1992), preceding the Selli Level and above the polarity zone correlative to CM0. The FO of *R. irregularis* is prior to CM0 and is followed by the FO of *N. truittii* (Fig. 12). Significant changes in nannoconid abundance at Gorgo a Cerbara are consistent with those detected in the Cismon core (Fig. 8). In particular, a sharp decline in abundance of narrow-canal nannoconids postdates the FO of *R. irregularis* and precedes CM0. In the upper part of CM0, the nannoconid abundance further decreases and wide-canal nannoconids outnumber the narrow-canal forms (Fig. 12).

SEDIMENTATION RATES

The identification of polarity chrons in the Cismon drill core and outcrop allow mean sedimentation rates within polarity chrons to be estimated. The age-depth plots for the drill core and coeval outcrop are comparable (Fig. 13), indicating consistent identification of polarity chrons. We use the CENT94 time scale (Channell et al., 1995a) for the age of polarity chron boundaries. Sedimentation rates are variable within the section (Table 3). Mean sedimentation rates within polarity chrons range from 5–12 m/m.y. in the upper 70 m of the drill core, to 3–8 m/m.y. in the 70–80 m interval characterized by reddish pseudonodular limestones. In the lower 35 m of the recovered section, average sedimentation rates increase to 30–70 m/m.y. (see Table 3; Fig. 13). In other Italian sections, the sedimentation rates in the CM0–CM2 interval are also variable, showing no consistent trends that might indicate time scale problems (Table 4; Fig. 13).

Whole-core volume magnetic susceptibility values in the Cismon drill core are generally positive, with 12 negative (diamagnetic) values in the 2339 values recorded downcore. Two intervals of higher ($\sim$20–60 $\times$ 10^{-6} SI) susceptibility were recorded in the 5–8 m and 73–80 m intervals (Fig. 4), and correspond to lithostratigraphic units 2 and 6, respectively. Unit 2 is a reddish limestone-marlstone-chert unit and unit 6 is a reddish pseudonodular unit. The higher susceptibilities are associated with the only two reddish intervals in the drill-core stratigraphy. The red color is undoubtedly attributable to pigmentary hematite (see

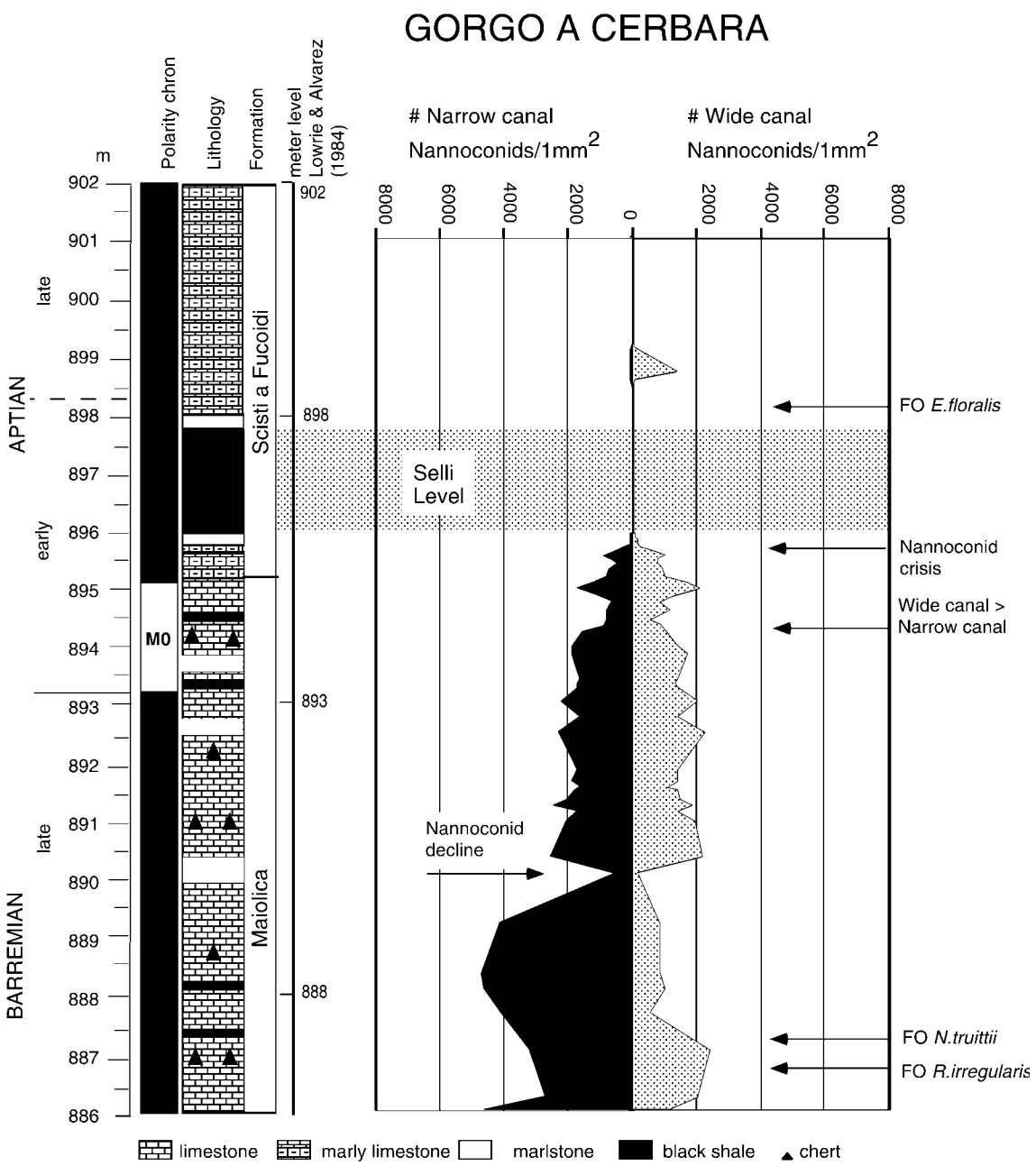

Figure 12. Gorgo a Cerbara: absolute abundance (number of specimens per square millimeter of thin section) of narrow- and wide-canal nannoconids in the vicinity of CM0. Other first occurrence (FO) datums are indicated.

Channell and McCabe, 1994); however, there is no evidence that hematite contributes to the NRM (see Figs. 2 and 5). The higher susceptibilities in the 5–8 m and 73–80 m intervals may be due to the presence of pigmentary (largely superparamagnetic) hematite, to iron-rich clay minerals, or to enhanced preservation of fine-grained magnetite in the reddish (more oxidized) intervals. The reddish interval at 73–80 m has a lower sedimentation rate (Fig. 13; Table 3) based on identification of polarity chrons, and we suspect that lower sedimentation rates also characterize the 5–8 m interval. The lower sedimentation rates would enhance oxidation of organic matter at the sediment-water interface, thereby retarding the reduction of sulfate to sulfide during early diagenesis. This, in turn, would minimize the dissolution (reduction) of fine-grained magnetite (to iron sulfide) and would allow fine-grained pigmentary hematite to grow, possibly from a goethitic or clay mineral precursor (see Channell et al., 1982). Spectral analysis of the magnetic susceptibility record (Fig. 4), either in the depth domain or when placed on the CENT94 time scale (Channell et al., 1995a), indicates no significant power peaks. In contrast, Mayer (1999) deduced the presence of 45, 80, and 180 cm cycles (which he attributed to orbital precession, obliquity, and eccentricity) in the susceptibility and percent carbonate record from a 8.5 m section in the CM10N to CM8 interval at Cismon.

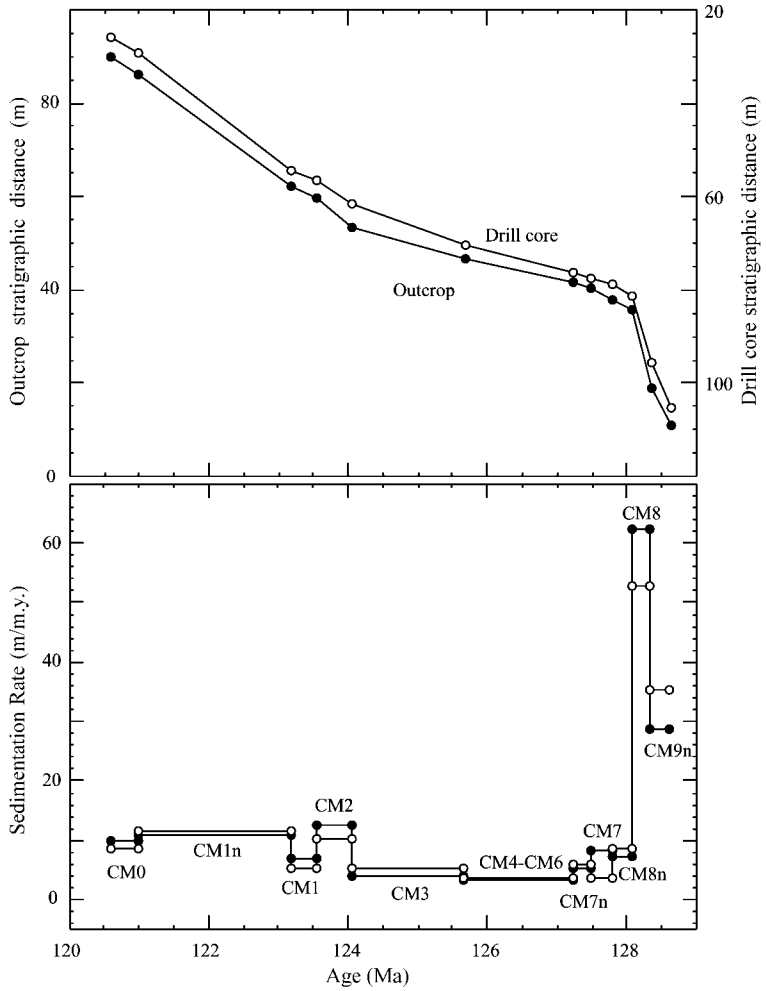

Figure 13. Stratigraphic distance (above) and interval sedimentation rates (below) plotted against age for the drill core and outcrop (lower and upper outcrops combined) based on the polarity chron designations and age of polarity chrons from the CENT94 time scale of Channell et al. (1995a).

TABLE 4. SEDIMENTATION RATES IN THE CM0–CM2 INTERVAL FOR VARIOUS ITALIAN MAIOLICA SECTIONS USING THE CENT94 TIME SCALE

Polarity chron	Cismon (core)	Cismon (outcrop)	Gorgo a Cerbara	Pie' del Dosso	Presale
CM0	8.6	10.0	5.0	6.4	3.3
CM1n	11.7	11.0	9.9	5.1	8.5
CM1	5.2	6.8	12.2	11.7	14.7
CM2	10.3	12.7	21.6		14.6
Reference	This paper	This paper	This paper and Lowrie and Alvarez (1984)	Channell and Erba (1992)	Lowrie and Alvarez (1984)

Note: Sedimentation rates given in m/m.y.

CONCLUSIONS

The polarity zone pattern at Cismon is not an unambiguous fit to the geomagnetic polarity time scale (GPTS) due to nonuniform sedimentation rates. The interpretation of polarity chrons in the Cismon drill core is facilitated by the recognition of 10 nannofossil events that have consistent correlation to polarity chrons in other Italian land sections and in deep-sea cores. In the 70–76 m interval of the drill core, correlated to the CM4–CM6 interval, the mean sedimentation rate drops to ~3 m/m.y. and the polarity chron pattern is not resolved. The low sedimentation rates in this interval are manifest by an interval of reddish nodular limestones within the gray pelagic limestones (Fig. 4). Close to the base of the drill-core section, within CM8, mean sedimentation rates are ~50 m/m.y. The polarity stratigraphy in the adjacent outcrop has been determined over the stratigraphic interval coeval with the drill core, allowing unequivocal correlation of the drill core to the outcrop. The proposed Barremian–Aptian boundary stratotype section at Gorgo a Cerbara has been resampled in the vicinity of CM0. Standard and newly proposed nannofossil events facilitate correlation to Cismon and improve stratigraphic control in the vicinity of the stage boundary.

ACKNOWLEDGMENTS

This research was supported by the U.S. National Science Foundation (grant EAR-9406424) and the Italian Consiglio Nazionale delle Ricerche (grant CT97.00285.CT05 to I. Premoli Silva). We appreciate the help of Roger Larson and our other APTICORE collaborators. We thank Kainian Huang for laboratory assistance, and John Stamatakos and Luca Lanci for reviews of the manuscript.

REFERENCES CITED

Bralower, T.J., 1987, Valanginian to Aptian calcareous nannofossil stratigraphy and correlation with the upper M-sequence magnetic anomalies: Marine Micropaleontology, v. 11, p. 293–310.

Bralower, T.J., Arthur, M.A., Leckie, R.M., Sliter, W.V., Allard, D.J., and Schlanger, S.O., 1994, Timing and paleoceanography of oceanic dysoxia/anoxia in the late Barremian to early Aptian: Palaios, v. 9, p. 335–369.

Cande, S.C., and Kent, D.V., 1992, A new geomagnetic polarity timescale for the Late Cretaceous and Cenozoic: Journal of Geophysical Research, v. 97, p. 13917–13951.

Cecca, F., Pallini, G., Erba, E., Premoli-Silva, I., and Coccioni, R., 1994, Hauterivian–Barremian chronostratigraphy based on ammonites, nannofossils, planktonic foraminifera, and magnetic chrons from the Mediterranean domain: Cretaceous Research, v. 15, p. 457–467.

Channell, J.E.T., and Erba, E., 1992, Early Cretaceous polarity chrons CM0 to CM11 recorded in northern Italian land sections near Brescia: Earth and Planetary Science Letters, v. 108, p. 161–179.

Channell, J.E.T., and McCabe, C., 1994, Comparison of magnetic hysteresis parameters of unremagnetized and remagnetized limestones: Journal of Geophysical Research, v. 99, p. 4613–4623.

Channell, J.E.T., and Medizza, F., 1981, Upper Cretaceous and Paleogene magnetic stratigraphy and biostratigraphy from the Venetian (Southern) Alps: Earth and Planetary Science Letters, v. 55, p. 419–432.

Channell, J.E.T., Lowrie, W., and Medizza, F., 1979, Middle and Early Cretaceous magnetic stratigraphy from the Cismon section, northern Italy: Earth and Planetary Science Letters, v. 42, p. 133–166.

Channell, J.E.T., Freeman, R., Heller, F., and Lowrie, W., 1982, Timing of diagenetic hematite growth in red pelagic limestones from Gubbio (Italy): Earth and Planetary Science Letters, v. 58, p. 189–201.

Channell, J.E.T., Bralower, T.J., and Grandesso, P., 1987, Biostratigraphic correlation of Mesozoic polarity chrons (M1 to CM23) at Capriolo and Xausa (South-

ern Alps, Italy): Earth and Planetary Science Letters, v. 85, p. 203–321.

Channell, J.E.T., Erba, E., and Lini, A., 1993, Magnetostratigraphic calibration of the late Valanginian carbon isotope event in pelagic limestones from northern Italy and Switzerland: Earth and Planetary Science Letters, v. 118, p. 145–166.

Channell, J.E.T., Erba, E., Nakanishi, M., and Tamaki, K., 1995a, A Late Jurassic–Early Cretaceous timescale and oceanic magnetic anomaly block models, *in* Berggren, W.A., Kent, D.V., Aubry, M.P., and Hardenbol, J., Geochronology, timescales, and stratigraphic correlation: SEPM (Society for Sedimentary Geology) Special Publication 54, p. 51–63.

Channell, J.E.T., Cecca, F., and Erba, E., 1995b, Correlations of Hauterivian and Barremian (Early Cretaceous) stage boundaries to polarity chrons: Earth and Planetary Science Letters, v. 134, p. 237–252.

Cita, M.B., and Gartner, S., 1973, Studi sul Pliocene e sugli strati di passaggio dal Miocene al Pliocene, IV. The stratotype Zanclean, foraminiferal and nannofossil biostratigraphy: Rivista Italiana Paleontologia Stratigrafia, v. 79, p. 503–558.

Coccioni, R., Erba, E., and Premoli-Silva, I., 1992, Barremian–Aptian calcareous plankton biostratigraphy from the Gorgo a Cerbara section (Marche, central Italy) and implications for plankton evolution: Cretaceous Research, v. 13, p. 517–537.

Erba, E., 1994, Nannofossils and superplumes: The Early Aptian nannoconid crisis: Paleoceanography, v. 9, p. 483–501.

Erba, E., 1996, The Aptian Stage, *in* Rawson, P.F., et al., eds., Proceedings of the 2nd International Symposium on Cretaceous Stage Boundaries: Bulletin de l' Institut Royal des Sciences Naturelles de Belgique, v. 66, supplement, p. 31–43.

Erba, E., and Larson, R.L., 1998, The Cismon Apticore (Southern Alps, Italy): A reference section for the Lower Cretaceous at low latitudes: Rivista Italiana Paleontologia Stratigrafia, v. 104, p. 181–192.

Erba, E., Channell, J.E.T., Claps, M., Jones, C., Larson, R., Opdyke, B., Premoli-Silva, I., Riva, A., Salvini, G., and Torricelli, S., 1999, Integrated stratigraphy of the Cismon Apticore (Southern Alps, Italy): A ''reference section'' for the Hauterivian–Aptian interval at low latitudes: Journal of Foraminiferal Research, v. 29, p. 371–391.

Helsley, C.E., and Steiner, M., 1969, Evidence for long intervals of normal polarity during the Cretaceous Period: Earth and Planetary Science Letters, v. 5, p. 325–332.

Kirschvink, J.L., 1980, The least squares lines and plane analysis of paleomagnetic data: Royal Astronomical Society Geophysical Journal, v. 62, p. 699–718.

Landra, G., Cecca, F., and Vasicek, Z., 2000, Early Aptian ammonites from the top of Maiolica and the anoxic ''Selli Level'' (Lombardy, Southern Alps): Bollettino Società Paleontologica Italiana, v. 39 (1),p. 29–45.

Larson, R.L., and Hilde, T.W.C., 1975, A revised time scale of magnetic reversals for the Early Cretaceous and Late Jurassic: Journal of Geophysical Research, v. 80, p. 2586–2594.

Lowrie, W., and Alvarez, W., 1984, Lower Cretaceous magnetic stratigraphy in Umbrian pelagic limestone sections: Earth and Planetary Science Letters, v. 71, p. 315–328.

Mayer, H., 1997, Magnetostratigraphy of Early Cretaceous Maiolica sections of the Southern Alps (Cismon and Pra da Stua, Italy): Geophysical Journal International, v. 131, p. 387–400.

Mayer, H., 1999, Calibration of the Early Cretaceous time scale by integration of magnetostratigraphy and cyclostratigraphy: Study of the Cismon Section (Southern Alps, Italy) and review: Neues Jahrbuch für Geologie und Paläontologie Abhandlungen, v. 212, p. 15–83.

McFadden, P.L., and McElhinny, M.W., 1990, Classification of the reversal test in paleomagnetism: Geophysical Journal International, v. 103, p. 725–729.

Thierstein, H.R., 1973, Lower Cretaceous calcareous nannoplankton biostratigraphy: Abhandlungen der Geologischen Bundesanstalt, v. A29, p. 1–52.

Thierstein, H.R., 1976, Mesozoic calcareous nannoplankton biostratigraphy of marine sediments: Marine Micropaleontology, v. 1, p. 325–362.

MANUSCRIPT RECEIVED BY THE SOCIETY JUNE 14, 1999
REVISED MANUSCRIPT RECEIVED NOVEMBER 17, 1999
MANUSCRIPT ACCCEPTED NOVEMBER 17, 1999

Printed in the USA